JOURNAL OF OPTOELECTRONICS AND ADVANCED MATERIALS Vol. 8, No. 3, June 2006, p. 1180 - 1186

Combined experimental and theoretical investigation of multiple-nanosecond laser ablation of metals

M. STAFE*, C. NEGUTU, I. M. POPESCU
University "Politehnica" of Bucharest, Department of Physics, Spl. Independentei, nr. 313, Bucharest, 060042, Romania

A detailed understanding of the physical determinants of the ablation rate in the multiple-nanosecond regime is of key importance for technological applications. Here, experiments and theoretical modeling are employed to investigate the ablation of thick aluminium plates produced by intense, multiple-nanosecond laser pulses. Opto-acoustic experimental measurements indicate that the ablation rate decays exponentially with the number of consecutive laser pulses. To understand in detail this behavior, we developed a theoretical photo-thermal model in which the complex phenomena associated with laser ablation are accounted for as supplementary terms in the classical heat equation. The ablation is considered as a thermal evaporation process induced by laser-absorption into the sample. Ablation rate decreases with the number of laser pulses due to reduction of the incident laser intensity with lateral area of the drilled hole. The photo-thermal model proposed here is validated by the good agreement between the experimental and the theoretical ablation rate that is obtained by integrating numerically the heat equation.

(Received March 22, 2006; accepted May 18, 2006)

Keywords: Laser-ablation, Ablation rate, Photo-thermal model

1. Introduction

Nanosecond Pulsed Laser Ablation (NPLA) is a photo-thermal phenomenon consisting in material removal that is induced by the absorption of the laser energy into the irradiated sample. The energy absorbed at the metal surface is converted into heat in a very short time (i.e. $\approx 10^{13}$ s) at the pulse scale. The nanosecond-duration of the laser pulses determines a small value of the heat diffusion length and, consequently, a reduced dissipation of the heat beyond the volume that is ablated. The reduced dissipation of the heat causes a local rise of the temperature of the irradiated material, accompanied by melting and vaporization [1-8]. The local character of the ablation allows micropatterning with an accurate control of the quality and of the aspect ratio. In addition, the thermo-mechanical tensions and the defects induced into the volume of the processed material are small. Due to these attractive features NPLA is a powerful tool for micropatterning hard, brittle and heat-sensitive materials, being widely used for various technological applications [1,9-12].

The key parameter that must be measured and controlled during micropatterning by NPLA is the ablation rate, which is the thickness of material layer ablated during a laser pulse. Several experimental techniques have been proposed that allow the ablation rate to be measured but not controlled [13-18]. These experimental approaches, while allowing for the ablation rate to be measured, do not provide any information about the actual phenomena involved in ablation process such as to predict the evolution of the process. A detailed understanding of NPLA requires theoretical modeling.

Ideally, an accurate theoretical description of the ablation process requires a heat equation that derives from the classical heat equation such as to accounts for all phenomena involved in the laser-matter interaction. Due to the complexity of the equation and to the time consume for its numerical integration, usually only a part of these phenomena are accounted for [1,19]. Thereby, the classical heat equation is developed with several supplementary terms only, depending on the irradiation regime that is considered, as follows. The heat source for the irradiated sample (i.e. the laser spot) and the lost of laser energy into the emerging plasma plume are described by the source term of the heat equation. The recession of the irradiated surface due to ablation is treated as a supplementary first-order spatial derivative term in the classical heat equation. The heat spent for melting and vaporization of a material layer is added to the term that describes the heating of the sample.

By integrating numerically the heat equation the temperature distribution within the irradiated material can be obtained, which allows for the ablation rate to be determined [20,21]. The previous models proposed for calculation of the ablation rate in nanosecond regime took into account the single pulse irradiation regime only [1,2,22]. This case is seldom employed in technological applications, which reduces the applicability of these models in predicting the evolution of the ablation process.

The ablation rate in the multiple-nanosecond regime is determined here by employing a combined experimental and theoretical approach. The experiments are performed using a real-time method for measuring and control the ablation rate during laser processing. The method is based on acoustic detection of the shock waves that emerge into the irradiated target. The experiments reveal that the ablation rate and the sample thickness decrease

exponentially with the number of laser pulses incident on the same spot. To explain this behavior we propose a photo-thermal model that accounts for the decrease of incident laser-intensity with lateral area of the ablated hole. The heat equation corresponding to this model is numerically integrated through finite elements method. The computed temperature-distribution within the target gives the surface recession velocity due to evaporation, and consequently the ablation rate. The simulation results indicate that the ablation rate and the sample thickness decrease exponentially with the number of consecutive laser pulses. The coefficients of the experimental and theoretical exponential functions describing variation of the sample thickness with the number of laser pulses are in good agreement, indicating that the model represents a good description of the phenomena involved in NPLA.

2. Experiment

The experimental setup used for real-time determination of the ablation rate is schematically depicted in Fig. 1a. The processing pulsed-laser beam is emitted from a "Brilliant" Q-switched Nd-YAG laser system provided with a second harmonic module generator. Laser pulses have the duration $\tau_p = 4.5$ ns, the repetition rate $\nu_p = 10$ Hz and the average energy per pulse of $E = 180$ mJ at $\lambda = 532$ nm. The laser pulses were fired through a lens system which can focus the laser beam to a spot-width of $2w = 0.3$ mm, such as to obtain an average intensity of 10^9 W/cm^2 on the irradiated sample surface. The sample consists of a 1 mm thick aluminium plate fixed on the lens focus, the piezoelectric detector being in direct contact with the sample in epicenter position relative to the laser spot.

The shock wave produced at the irradiated surface by the recoil of the laser-induced plasma propagates through the sample with a velocity equal to that of the sound in aluminium (6300 m/s) and produces a displacement of the opposite sample-surface. The piezoelectric detector produces an electric signal response that is digitally acquired on the oscilloscope whose time base is triggered by a photodiode (Fig. 1a) that captures a part of the light scattered on the incidence sample-surface. The signal is further analyzed using a computer.

The propagation time of the shock-wave through the sample is given by the interval between the former peak of the triggering photodiode signal and the first peak from the acoustic detector signal (Fig. 1b). The interval variation of 0.1 ns detectable on the oscilloscope corresponds to a sample thickness variation, and an ablation-rate, of 0.3 μ m/pulse.

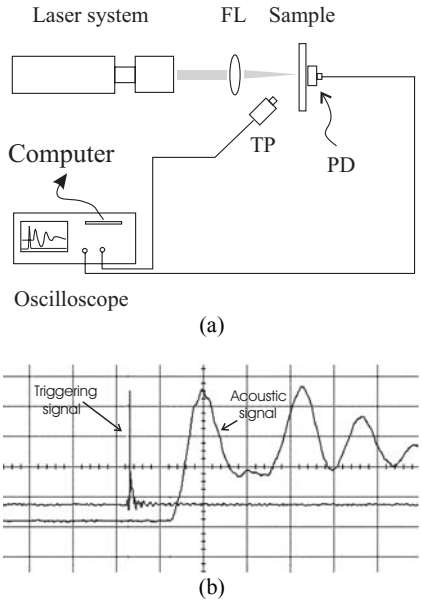

Fig. 1. (a) Experimental setup for real-time determination of the ablation rate. FL is the focusing lens, TP- triggering photodiode, and PD- the piezoelectric detector. (b) Electric signals from the acoustic detector and triggering photodiode as captured on oscilloscope. The time scale is 200 ns/div.

3. The ablation photo-thermal model

The photo-thermal model presented here is based on the observation that the laser light is almost exclusively absorbed by the conduction-band electrons in metals, resulting in intraband transitions [1,9]. Thermalization of the absorbed energy is mainly achieved through electron-electron collisions, with a relaxation time in the order of $10^{11} \div 10^{12}$ s. Therefore, the thermalization of the absorbed laser energy is a very fast process at the nanosecond laser pulses scale. Thus, the laser spot on the sample surface can be considered as a simple heat source.

The heat flow propagates inside of the sample and heats the material. Dimensionality of the heat flow and of the heat equation is determined by the size of the heat diffusion length l_T

$$l_T = 2\left(D\tau_p\right)^{1/2} \tag{1}$$

relative to other characteristic lengths, such as the radius w of the processing laser beam, the optical penetration depth $l_\alpha = \alpha^{-1}$, and the thickness of the sample, h_s. D is the thermal diffusivity and S is in the experiment employed here, the values of these parameters are $l_T = 1.3$ μm, $l_\alpha = 0.006$ μm, $2w$=300 μm and $h_s = 1$ mm. These values satisfy the relation

$$l_\alpha << l_T << w, h_s \tag{2}$$

that describes a strong light absorption into the material, a negligible lateral heat flow, and a semi-infinite sample. As a consequence, the temperature distribution in the axial z direction can be obtained from the one-dimensional heat equation.

4. The heat equation

The one-dimensional heat equation describing the propagation of heat flow into the irradiated sample can be written as [1,20,21]:

$$\rho c_p\left(\frac{\partial T}{\partial t}-v_a\frac{\partial T}{\partial z}\right)-k\frac{\partial^2 T}{\partial z^2}=Q(z,t) \tag{3}$$

where ρ, c_p and k denote the density, the specific heat, and respectively the thermal conductivity of the metalic material, taken as constant, temperature-independent parameters. v_a is the recession velocity of the irradiated surface due to ablation. Position of this surface is labeled with $z=0$ in a coordinates system that is fixed to the receding surface.

The source term $Q(z,t)$ describes the laser energy absorbed into the sample, per unit volume and time, that is converted into heat [1,2]:

$$Q(z,t)=[1-R(\lambda)]\alpha I(t)\exp\left(-\int_0^t \alpha_{pl}v_{pl}dt\right) \tag{4}$$

where $R(\lambda)$ denotes the wavelength-dependent normal reflectivity at the processed area, and α denotes the aluminium absorption coefficient. The laser intensity

$$I(t)=I_0\frac{t}{\tau_p}\exp\left(1-\frac{t}{\tau_p}\right) \tag{5}$$

describes the smooth profile of the laser pulses emited from the laser system. The peak intensity I_0 is calculated such as the time integral of $I(t)$, multiplied with the incidence area, to give the mean energy of the laser pulse of 180 mJ. α_{pl} in (4) states for the absorption coefficient of the laser beam into the vapour plume (that expands away from the target with velocity v_{pl}) before reaching the sample surface.

The laser energy absorbed into the sample melts a metallic layer whose depth h_m at a moment t is determined by the coordinate z satisfying the condition

$$T(z,t)\geq T_m\,. \tag{6}$$

Above the melt surface having temperature T_s the saturated vapor pressure p_s is given by the Clausius-Clapeyron equation [1,2,7]:

$$p_s=p_0\exp\left[\frac{M\Delta H_v(T_b)}{k_B}\left(\frac{1}{T_b}-\frac{1}{T_s}\right)\right], \tag{7}$$

where $\Delta H_v(T_b)$ is the vaporization enthalpy at normal boilling point T_b, $p_0=1$ atm, M denotes the atomic mass of aluminium, and k_B is the Boltzmann constant.

Due to the high laser-intensity, the vapour ionizes rapidly during the first part of the laser pulse and becomes a plasma that absorbs further the laser beam via electron-ion inverse Bremsstrahlung mechanism. This is the dominant absorption mechanism in the plume during the laser pulse [5,23]. For the sake of simplicity, the plasma plume is considered uniform in space. The absorption coefficient α_{pl} (in cm^{-1}) of the plasma is related to the surface temperature via the ions density (N_i in cm^{-3}), the electrons density (N_e in cm^{-3}), and the plasma temperature T_{pl} [1,11]:

$$\alpha_{pl}=C\frac{\lambda^3 Z^2 N_i N_e}{T_{pl}^{1/2}}\left[1-\exp\left(-\frac{\hbar\omega}{k_B T_{pl}}\right)\right] \tag{8}$$

where $C=1.37\times10^{-35}$, λ (in μm) denotes the laser wavelength, ω represents the laser frequency, Z is the average ionic state, and $\hbar$ is the Plank constant. In the case where plasma is considered an ideal single-particle gas, with specific heat ratio $\gamma=5/3$, the ions and electrons number densities are given by

$$N_i\cong N_e=0.31\frac{p_s}{k_B T_{pl}} \tag{9}$$

and the plasma hydrodynamic velocity is equal to the sound velocity within the aluminium vapor atmosphere:

$$v_{pl}=\left(\gamma k_B T_{pl}/M\right)^{1/2} \tag{10}$$

where the plasma temperature is given by the relationship

$$T_{pl}=0.67T_s \tag{11}$$

Therefore, the maximum velocity of the evaporation front, i.e. the ablation velocity, is given by the Hertz-Knudsen equation [1,2]:

$$v_a=v_{ev}=0.32\left(\frac{M}{k_B T_s}\right)^{1/2}\frac{p_s}{\rho} \tag{12}$$

and the ablation rate is given by time integral of the evaporation-front velocity:

$$\Delta h=\int_0^{1/\nu_p} v_a dt\,. \tag{13}$$

The correction coefficients 0.31 in eq. (15), 0.67 from eq. (17) and 0.32 in (8) were introduced such as to account for the influence of the Knudsen layer on the plasma parameters [1,2].

Thus, the ablation rate may be determined by computing the temporal evolution of the sample-surface temperature. The dependence of the ablation velocity v_a and plasma absorption coefficient α_{pl} to the sample surface temperature T_s leads to difficulties in solving the heat equation. The solution to this problem is to use a multi-step method for integrating of the heat equation (3).

5. Boundary and initial conditions

Due to the small thermal relaxation time ($\tau_T\approx w^2/k=10^{-5}$ s) relative to the interval between two consecutive laser pulses ($1/\nu_p=0.1$ s), the surface irradiated by a laser pulse is cooled to the initial temperature T_{amb} before the beginning of the next pulse

[18]. Thus, **the initial condition** at the beginning of each successive laser pulse is

$$T(z)\big|_{t=0} = T_{amb}. \quad (14)$$

The boundary condition at the irradiated surface (i.e., at $z = 0$), giving the energy balance, is [1,2,21]

$$-k\frac{\partial T}{\partial z}\bigg|_{z=0} = -J_{phase} - J_{loss} \quad (15)$$

Due to the small thermal penetration depth l_T relative to the sample thickness h_s, a constant-temperature boundary condition is used for the surface opposite to that irradiated ($z = h_s$):

$$T\big|_{z=h_s} = T_{amb} \quad (16)$$

In the boundary condition (19)

$$J_{phase} = \rho v_a \left[\Delta H_m(T_m) + \Delta H_v(T_b)\right] \quad (17)$$

denotes the energy flux which determines the melting and vaporizing of the ablated layer during the laser pulse,

$$J_{loss} = \eta(T_s - T_{amb}) + \sigma_r \varepsilon_t \left(T_s^4 - T_{amb}^4\right) \quad (18)$$

is the energy flux into the ambient medium produced by surface conductance and thermal radiation, η denotes the surface conductance, ε_t is the total emissivity, $\sigma_r \cong 5.7\times10^{-12}$ W/(cm^{2}K^4) is the Stefan-Boltzman constant, $\Delta H_m(T_m)$ is the melting enthalpy at normal melting point T_m.

Integration of the heat equation for the period corresponding to a laser pulse is performed through a multi-step method, in which the result of an integration step is used as input for the next integration step. The value of the time-step is $\Delta t_{step} = 10^{-11}$ s, ensuring the convergence of the solution. The sum of the *N* time-steps gives the laser-pulses period

$$1/\nu_p = N\Delta t_{step}. \quad (19)$$

For the first integration step of a laser pulse, the recession (ablation) velocity of the irradiated surface v_a, the plasma velocity v_{pl}, and the plasma absorption coefficient α_{pl} are set to zero. The initial condition for the first step is (14), while the boundary conditions are given by (15) and (16). The heat equation is integrated through the finite differences method [7,21], using the values of the thermal and optical parameters given in *Table I* [1].

The calculated temperature distribution within the sample at the end of the first step, $T(z)\big|_{t=\Delta t_{step}}$, is used as the initial condition for the second integration step. The surface temperature gives the "instantaneous" values of the plasma absorption coefficient α_{pl}, plasma velocity v_{pl}, and recession velocity of the sample-surface v_a during the first time-step.

Table 1. Thermal and optical properties of Al.

Property	Symbol	Value
Surface conductance	η	10^{-4} W/cm^{2}K
Total emissivity	ε_t	0.4
Melting temperature	T_m	933 K
Boiling temperature	T_b	2730 K
Melting enthalpy	ΔH_m	410 J/g
Vaporization enthalpy	ΔH_v	10750 J/g
Density	ρ	2.7 g/cm^3
Specific heat	c_p	0.90 J/gK
Thermal conductivity	k	2.37 W/cmK
Thermal diffusivity	D	1.5 cm^2/s
Reflection coefficient	R	0.92(532 nm)
Absorption coefficient	α	1.5×10^6 cm^{-1}

These values of the ablation velocity and plasma absorption coefficient are introduced as parameters in the heat equation (3), and into the expression J_{phase} from the boundary condition (15) for the second integration step.

The heat equation is integrated for the remaining time steps of the laser pulse following the same procedure as for the first step.

6. Results and discussion

The time evolution of the irradiated-surface temperature and the dependence of the ablation rate on the number of consecutive laser pulses were investigated using the photo-thermal model introduced above. The temperature of the sample surface in the single and multiple pulse irradiation regimes obtained by integrating the heat equation is given in Fig. 2.

The surface temperature increases to its maximum in about 1.5 ns, following the intensity-profile of the laser beam that is incident on the sample surface (Fig. 2a), indicating the process of coupling and decoupling of the laser energy to the substrate. Thus, during the first part of the laser pulse the entire laser energy is coupled to the sample surface because the plasma ionization degree and the absorption coefficient is approximately zero. As a consequence, the surface temperature increases rapidly to a peak value of ≈ 15000 K (Fig. 2a). This leads to a large value for the plasma density and ionization degree, and consequently to the increase of the inverse Bremsstrahlung absorption coefficient. The total laser energy coupled to the substrate during a laser pulse represents only $\approx 30\%$ from the total energy, the rest of the energy being absorbed into the plasma plume. Therefore, the surface-temperature decreases during the next time steps of the laser pulse and reaches the ambient temperature in about 70 ns (Fig. 2a).

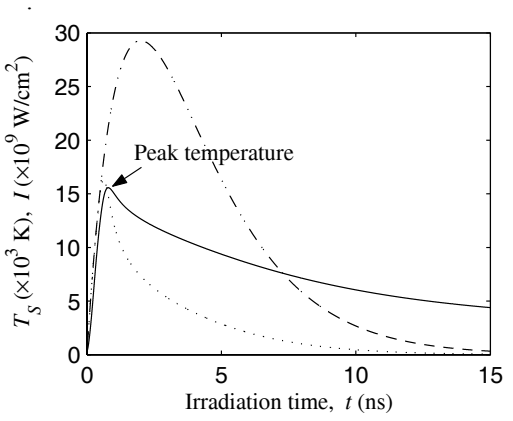

(a)

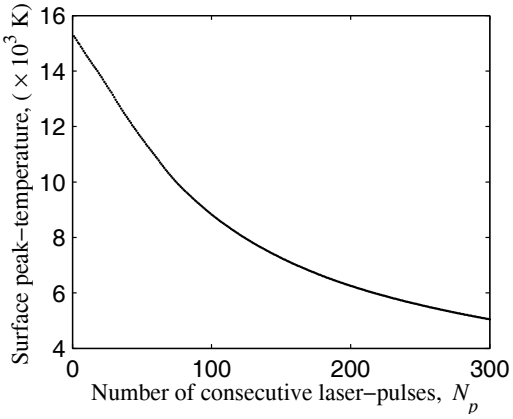

(b)

Fig. 2. (a) Surface-temperature T_s (solid line), non-attenuated beam-intensity profile (dash-dotted line), and plasma-attenuated beam profile (dotted line) during a laser pulse. (b) Surface peak-temperature as a function of consecutive laser pulses number.

The peak temperature of the sample surface progressively decreases from 15000 K to about 3000 K as the number of the laser pulses increases to 300 (Fig. 2b). This behavior of the surface temperature reflects the decreasing of the laser intensity due to increasing of the crater lateral-area. The crater is approximated by a circular paraboloid due to the Gaussian spatial-distribution of the laser intensity. The characteristics of the paraboloidic crater are the base radius w, the height h_c and the lateral are A_c. At the end of the integration cycle corresponding to a laser pulse, the crater height h_c, the sample thickness h_s, the incidence-area of the laser-beam A_c, and the peak-intensity I_0 of the laser beam are recalculated to the values:

$$h_c + \Delta h \to h_c';\qquad h_s - h_c \to h_s';$$
$$A_c(h_c) = \frac{\pi w\left[\left(w^2 + 4h_c^2\right)^{3/2} - w^3\right]}{6h_c^2} \to A_c'(h_c) \tag{20}$$

$$E = \int_0^{1/\nu_p} I(t)\tau_p A_c\,dt \to\ E = \int_0^{1/\nu_p} I(t)\tau_p A_c'\,dt$$

where $I(t)$ is given by (5) and E is the laser pulse energy. As a result, the area irradiated by the laser beam during the next laser pulse increases and the intensity I of the laser beam decreases as compared to the previous pulse. Integrating the heat equation for each successive laser pulse in these conditions, the surface peak-temperature and the ablation rate corresponding to a given laser pulse decrease as compare to the previous pulse. Therefore, the peak-intensity of the laser beam at the sample-surface decays from $\approx 3\times10^{10}$ W/cm^2 in the case of former pulse to $\approx 10^9$ W/cm^2 in the case of last pulse, while the ablation rate Δh decreases from $\approx 2\,\mu$m/pulse to less than 0.5 μ m/pulse (Fig. 3a). Following the procedure described above, the variation of the sample thickness with the number of laser pulses incident on the sample surface is also computed (Fig. 3b).

The computed points in Fig. 3b, representing the variation of the sample thickness with the pulses number, were fitted with an exponential function:

$$h_s = 0.59 + 0.41\exp\left(-N_p/198\right)(\text{mm}) \tag{21}$$

The dependence of the sample thickness on the number of laser pulses as given by the experiment described in section 2 is plotted in Fig. 3c. The exponential curve obtained by least-squares fitting is described by

$$\begin{aligned} h_s &= h_f + \left(h_i - h_f\right)\exp\left(-2N_p/N_{th}\right) \\ &= 0.62 + 0.36\exp\left(-N_p/120\right)(\text{mm}) \end{aligned} \tag{22}$$

where the threshold value for the number of consecutive laser pulses corresponding to a zero ablation rate is $N_{th} = 240$; h_i and h_f are the initial and respectively the final thickness of the sample.

There is a reasonable agreement between the values of the parameters in the fitting equations (21) and (22). The differences between the values of the theoretical and the experimental fitting parameters h_f and N_{th} indicate a slower installation of the saturation in the case of theoretical fitting curve (Fig. 3b,c), which may be due to the simplifying hypothesis of freely expanding plasma (10). This assumption is correct only during the first laser pulses. As the number N_p of laser pulses and the hole's depth h_c increase, there is a reduction of the expansion velocity of the plasma plume. This would lead to a rapid increase of the plasma temperature and of the absorption coefficient during a final laser pulse, and consequently to a weaker coupling of the laser energy to the substrate.

Further calculations will be performed to investigate this hypothesis.

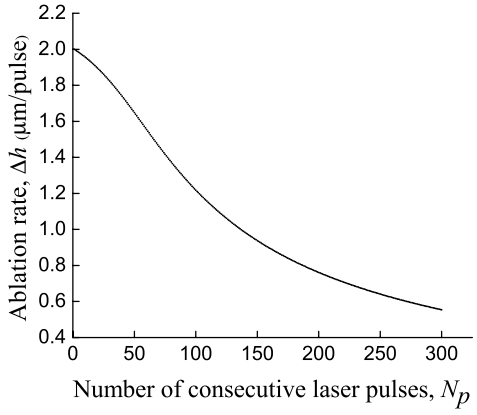

(a)

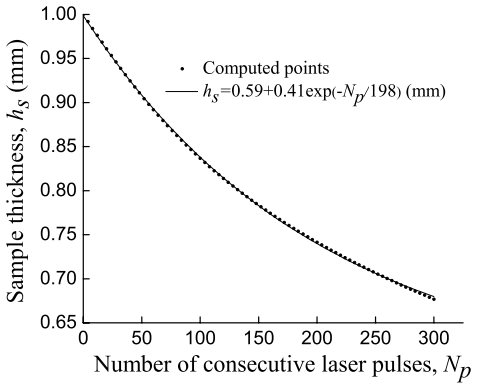

(b)

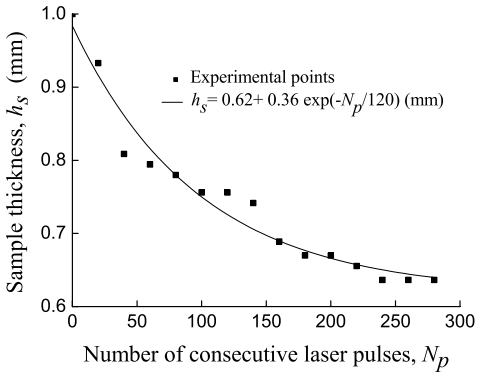

(c)

Fig. 3. (a) Ablation rate as a function of laser-pulses number. The computed (b) and experimental (c) points that represent the variation of the sample thickness with the number of consecutive laser pulses. The solid lines represent the fitting curves.

7. Conclusions

Theory and experiments were combined to determine the ablation rate in the case of NPLA of a thick aluminium plate. The experimental ablation rate was obtained by using a real-time method for determining the sample thickness involving the direct detection of the resulted shock waves into the aluminium plate by using acoustic detectors. The experimental data indicate an approximately exponential decrease of the sample thickness and of the ablation rate as the number of laser pulses increases.

A photo-thermal model was proposed that allows the numerical determination of the ablation rate in NPLA conditions. In this model, the vaporization proceeds from a transient liquid phase that may be super-heated beyond the critical point due to the recoil pressure exerted by the expanding plasma plume and to the rapid coupling of the laser energy to the sample. By considering the absorption of the incoming laser energy into the plasma plume produced above the sample surface, we demonstrated that only approximately 30% of the laser pulse energy is coupled to the substrate. Plasma absorption and phase transitions were taken into account through the boundary conditions of the heat equation. The initial conditions account for the decrease of the laser intensity at the irradiated surface at the beginning of each consecutive laser pulse due to the increase of the depth and inner area of the parabolic hole produced during NPLA. The temperature distribution within the aluminium sample, the surface temperature as a function of time, and the corresponding evaporation velocity were calculated by solving the one-dimensional heat equation.

The ablation rate was obtained by integrating over time the ablation velocity function, while the sum over all pulses of the ablation rates gives the hole depth and the sample thickness. The computed ablation rate and sample thickness decrease exponentially as the number of consecutive laser pulses increases. The good agreement between the parameters of the computed and experimental fitting curves describing the variation of the sample thickness with the number of laser pulses indicates the validity of the theoretical model presented here.

Acknowledgement

Partial financial support was provided by the Romanian Ministry for Research and Technology (MCT) in the framework PNCDI 2003 (grant CERES 3-107). We thank A. Toma and A. Harabor for technical assistance and useful advice.

References

[1] D. Bauerle, Laser processing and chemistry, Springer-Verlag, Berlin Heidelberg, 2000.
[2] A. Peterlongo, A. Miotello, R. Kelly, Phys. Rev. E**, 50**, 161 (1996).
[3] I. Ursu, I. N. Mihailescu, A. M. Prokhorov, V. I. Konov, Interactiunea radiatiei laser cu metalele, Ed. Acad. RSR, Romania, 1986.
[4] S. Amoruso, Appl. Phys.A, **69**, 314 (1999).
[5] E. G. Gamaly, A. V. Rode, A. Perrone, A. Zocco, Appl. Phys. A **73**, 143 (2001)

[6] E. G. Gamaly, A. V. Rode, B. Luther-Davies, J. Appl. Phys. **85**, 4213 (1999).
[7] R. K. Ganesh, W. W. Bowley, R. B. Bellantone, Y. Hahn, Journal of Computational Physics **125**, 4716 (1994).
[8] R. Niedrig, O. Bostanjoglo, J. Appl. Phys. **81**, 480 (1997).
[9] J. F. Ready, Efects of high-power laser radiation, Academic Press, New York, 1971.
[10] D. Bauerle, Proceedings of an International Conference- Laser Processing and Diagnostics, Springer-Verlag, Berlin, 1984.
[11] I. M. Popescu, G. F. Cone, A. M. Preda, P. E. Sterian, St. St. Tudorache, A. I. Lupascu, C. P. Cristescu, Aplicatii ale laserilor (roum.) (Laser applications), Ed. Tehnica, Bucuresti, 1979.
[12] G. Mourou, Appl. Phys. B, **65**, 205 (1997).
[13] S. Strgar, J. Mozina, Appl. Phys. A, **74**, 321 (2002).
[14] R. Pini, R. Salimbeni, M. Vannini, G. Toci, Appl. Phys. B, **61**, 505 (1995).
[15] M. Stafe, C. Negutu, I. M. Popescu, Shock waves **14**, 123 (2005).
[16] S. Strgar, J. Mozina, Ultrasonics **40**, 791 (2002).
[17] Z. Marton, P. Heszler, A. Mechler, B. Hopp, Z. Kantor, Z. Bor, Appl. Phys. A, **69**, 133 (1999).
[18] V. P. Zharov, V. S. Letokhov, Laser Optoacoustic Spectroscopy, Springer-Verlag, Berlin Heidelberg New York, 1986.
[19] M. von Allmen, A. Blatter, Laser-Beam Interactions with Materials, Springer-Verlag, Berlin, 1995.
[20] F. P. Incropera, D. P. Dewitt, Fundamentals of heat and mass transfer, John Willey and Sons, New York, 2002.
[21] L. D. Landau, E. M. Lifshitz, Fluid Mechanics, Pergamon Press, Oxford, New York, 1987.
[22] A. Vedavarz, K. Mitra, S. Kumar, J. Appl. Phys. **76**, 5014 (1994).
[23] F. J. Gordillo-Vasquez, A. Perea, J. A. Chaos, J. Gonzalo, C. N. Afonso, Appl. Phys. Lett. **78**, 7 (2001).
[24] H. Strehlow, Appl. Phys. A **72**, 45 (2001).

*Corresponding author: stafe@physics.pub.ro